

Neutron Diffraction Studies of Polycrystalline Ni/Mg/Al Mixed Oxides Obtained from Hydrotalcite-like Precursors

Massimo Gazzano,^{*,†} Winnie Kagunya,[‡] Davide Matteuzzi,[§] and Angelo Vaccari[§]

Centro per lo Studio della Fisica delle Macromolecole-CNR, Via Selmi 2, 40126 Bologna (Italy), ISIS Facility, Rutherford Appleton Laboratory, Chilton, Didcot OX11 0QX, U.K., and Dipartimento di Chimica Industriale e dei Materiali, Università degli Studi, Viale Risorgimento 4, 40136 Bologna, Italy

Received: November 12, 1996; In Final Form: February 19, 1997[®]

The thermal decomposition of a synthetic hydrotalcite-type (HT) sample $[\text{Mg}_{0.71}\text{Al}_{0.29}(\text{OH})_2(\text{CO}_3)_{0.145} \cdot m\text{H}_2\text{O}]$ has been investigated by neutron diffraction using a programmed temperature control facility. The evolution from HT phase to mixed oxide leading ultimately to the partial segregation of a spinel phase is reported. Structural modification ascribed to the interlayer water loss from the HT phase is accompanied by a reduction of the *c*-axis parameter and changes in the neutron powder pattern. The neutron diffraction patterns of five Mg/Ni/Al mixed oxides obtained from HT samples by calcination at 923 K were subjected to structural refinement by the Rietveld method. The model that best describes the refined data consists of a supercell with an *a*-axis twice that of the stoichiometric rock-salt type oxide, a certain degree of ordered cation vacancies in the octahedral sites, and partially occupied tetrahedral sites. Although the samples essentially show the typical patterns of a rock-salt type structure, the results indicate that they conform to a spinel type structure, which corroborates the deductions made by workers using other techniques. A high replacement of aluminium for magnesium in the magnesium-richer samples is proposed.

I. Introduction

High surface-area homogeneous mixed oxides have many commercial applications, for example, as adsorbents, catalysts, and pigments and in sensor and magnetic technologies.^{1–4} Their preparation requires the application of synthesis procedures that ensure the intimate mixing of the components without the need for high-temperature treatments. Thermal decomposition of hydrotalcite-type anionic clays (HT) with the general formula $[\text{M}(\text{II})_{1-x}\text{M}(\text{III})_x(\text{OH})_2]^{x+}[\text{A}_{x/n}^{n-}]^{x-} \cdot m\text{H}_2\text{O}$ (where M is a metal cation and A an anion (usually carbonate)) at moderate temperatures fulfills these requirements.^{4–7} The level of interest in HT based on this composition is reflected by the large number of recent publications.^{8–11} The HT compounds obtained when $\text{M}(\text{II}) = \text{Mg}^{2+}$, $\text{M}(\text{III}) = \text{Al}^{3+}$, and $\text{A} = \text{CO}_3^{2-}$ are widely used as precursors of solid basic catalysts or catalyst supports. Although for this system the loss of water and anions following thermal treatment between room temperature (RT) and 773 K has been investigated previously using X-ray diffraction and spectroscopic techniques,^{9,10,12,13} additional studies aimed at extending this range to 1250 K are warranted in view of the possibility of generating the catalysts by calcination of HT samples also at relatively high temperatures.

From previous studies, the oxide phases obtained by calcination have been reported to have defective structures. The composition of the crystalline fraction and the location of the individual cations have not been conclusively determined and remain a matter of intense discussion.^{10,14–17} The reason behind the modification of the properties induced by increasing amounts of Mg^{2+} ions is of considerable interest, since MgO is found to be a promoter in commercial nickel catalysts. Studies of the effects of progressive dilution of the transition metal in Ni/Al

systems would give further understanding of the catalysts generated from HT systems. In addition, for the Mg/Al system, an increase of the Al^{3+} ion concentration has been reported to stabilize MgO toward sintering or crystallization, leading to potential applications for stabilized magnesia as basic catalysts or as a catalyst support.^{5,7} An example of this last application is the use as stabilized support for noble metals in $\text{C}_6\text{—C}_8$ aromatization.^{18,19}

Among the catalysts employed in hydrocarbon reforming and methane oxidation reactions are those based on Ni/Mg/Al mixed oxide systems.^{20–22} Based on a simple NiO lattice model, the limited substitution of aluminium atoms for nickel positions is evident in the Ni/Al mixed oxide component.¹⁵ Two different structural models have been proposed for Mg/Al mixed oxide by Rebours *et al.* in studies aimed at arriving at a better understanding of the location of cations and the nature of the active sites in the system:¹⁴ (i) aluminium-substituted MgO lattice in which Al atoms are statistically distributed over the Mg position; (ii) aluminium-substituted MgO lattice with the addition of metal atoms in the interstitial positions.

Previous studies have been directed toward estimating the occupancy factor of the metal sites using X-ray diffraction. Because of the small variation in the X-ray scattering factors of Mg^{2+} and Al^{3+} , the technique is limited in studies of Mg/Al systems. Neutron diffraction is complementary in this respect and has, therefore, been used to resolve a number of structural related problems. We report on its application in addressing a number of structural related problems, specifically, (i) the *in situ* temperature-programmed neutron diffraction analysis of a synthetic HT sample $[\text{Mg}_{0.71}\text{Al}_{0.29}(\text{OH})_2(\text{CO}_3)_{0.145} \cdot m\text{H}_2\text{O}]$ between RT and 1250 K and (ii) the refinements of the neutron diffraction profiles of five Ni/Mg/Al mixed oxide samples obtained from HT by calcination at 923 K.

II. Experimental Section

The HT samples were prepared by mixing with vigorous stirring a solution containing nitrate salts in a molar ratio $\text{M}(\text{II})/$

* Corresponding author. Fax: +39 51 259456. Telephone: +39 51 259549. E-mail: gazzano@area.bo.cnr.it.

[†] Centro per lo Studio della Fisica delle Macromolecole-CNR.

[‡] Rutherford Appleton Laboratory.

[§] Università degli Studi.

[®] Abstract published in *Advance ACS Abstracts*, April 15, 1997.

M(III) of 2.5 with a second solution containing a slight excess of NaHCO_3 . The pH was maintained at 8.0. The precipitates were kept in suspension at 333 K for 30 min and then filtered, washed (until the sodium content (as Na_2O) was lower than 0.02 wt %), and dried overnight at 363 K.^{15,17}

Neutron diffraction experiments were performed on the D2B diffractometer at the ILL-High Flux Reactor in Grenoble using a wavelength of 1.594 Å (from the Ge (3 3 5) reflection) at a resolution $\Delta d/d$ of 5×10^{-4} .²³ The angular coverage is $5 \leq 2\theta \leq 165$, and for the scans, a step size of 0.05° was used. The data for the room temperature scans were recorded for 6.5 h (corresponding to 320 000 neutron counts) in a vanadium sample holder. For the *in situ* temperature analyses, the Mg/Al sample was contained in a quartz cell containing two thermocouples that was then loaded into a furnace under automated control. The diffraction patterns were recorded for 3.5 h (corresponding to 150 000 counts) at the temperatures indicated in Figure 1. The same sample was used and before each scan, data collection was delayed for 0.5 h to allow temperature equilibration.

Background subtraction was performed using the diffraction patterns scanned at 700 K of a quartz cell containing the thermocouples after correction for peak shift due to thermal expansion. Data manipulation was carried out rigorously, since the intensity of the furnace was observed to be a major contribution to the total profile intensity.

III. Data Analysis

The full pattern refinements based on the Rietveld procedure^{24,25} were carried out using the PC version of the DBW-9006 program by Wiles and Young.²⁶ The neutron cross sections of Ni, Al, Mg, and O atoms²⁷ were used. A fourth- to sixth-order polynomial equation was employed to assimilate the background while the peaks were fitted with a pseudo-Voigt function.

In the first cycles the scale factor and the background coefficients were refined. Successively, the profile parameters (peak widths and their dependence on 2θ , true 2θ zero, Lorentian fraction) and the lattice parameters were allowed to vary too. Finally, the occupancy factors (OF) were refined, and the cation substitution was tested. The atomic displacement parameters (adp) were fixed at the values from single-crystal data for MgO and NiO²⁸ because of their strong correlation with the OF. The same adp were used for the different chemical species occupying the same location. Only at the end of the refinement procedures were some trials carried out using the reported Ni adp for Mg atoms and vice versa to assess the uncertainty in the OF due to inconsistencies in the adp. In all cases the variations induced in the OF from the change of the adp factors were minor or equal to the OF estimated standard deviations (esd).

IV. Results and Discussion

The need to increase our knowledge on the correlation between activity and the nature of the oxide phases in a situation as close to that used in catalytic devices as was practically possible motivated us to undertake this study. It is noteworthy that the neutron diffraction technique offers a far wider angular range than is available with X-ray diffraction. Owing to the absence of variations in the neutron-scattering factors with 2θ , the largest number of good intensity reflections was collected.

(a) *In Situ* Temperature-Programmed Experiments. The neutron diffraction powder patterns of the Mg/Al sample [$\text{Mg}_{0.71}\text{Al}_{0.29}(\text{OH})_2(\text{CO}_3)_{0.145} \cdot m\text{H}_2\text{O}$] heated *in situ* at different temperatures (Figure 1) reveal that a HT phase is the only crystalline product below 600 K. Between 700 and 1000 K, a cubic oxide

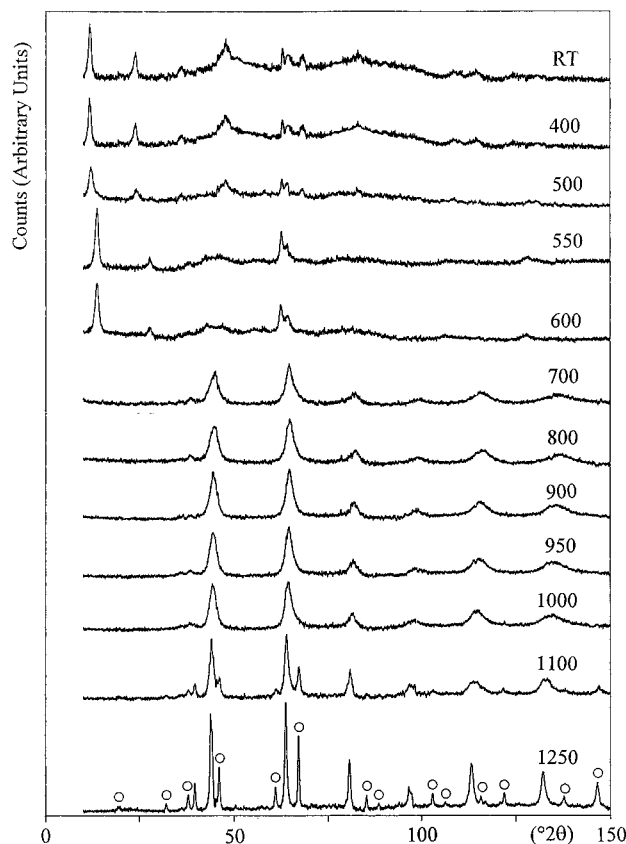


Figure 1. Neutron diffraction profiles of HT after *in situ* thermal treatment at various temperatures (see inset). Between RT and 600 K the peaks belong to HT-like phase and above this to MgO and spinel phases. Where present, these are labeled with a circle.

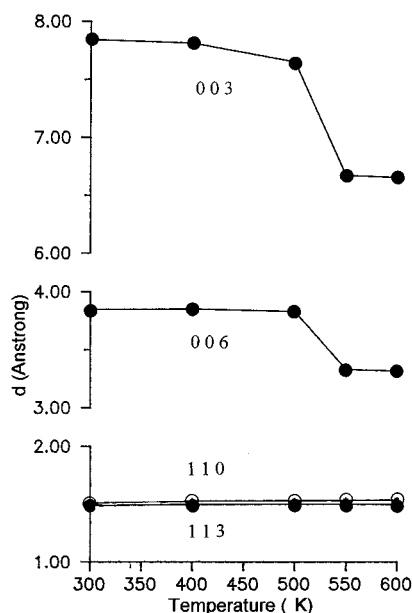


Figure 2. *d*-Spacing values corresponding to the indicated planes as a function of the temperature for the Mg/Al sample calcined *in situ*.

phase isomorphous to MgO is present. It converts partially to the spinel phase between 1100 and 1250 K. Although the diffraction patterns in Figure 1 show a high level of background noise due to poor crystallinity and coherent hydrogen scattering, the structural modification that the HT phase undergoes during calcination is evident from the variation in the position and intensity of the most prominent peaks.

From the plots in Figure 2 it is observed that the *d*-spacings of the two reflections (0 0 3) at $2\theta = 11.8^\circ$ and (0 0 6) at $2\theta =$

TABLE 1: Phase Evolution with the Temperature and Lattice Parameters for the Mg/Al Sample As Deduced from Neutron Diffraction Spectra^a

	temperature (K)											
	RT	400	500	550	600	700	800	900	950	1000	1100	1250
phase	HT	HT	HT	HT	HT	O	O	O	O	O	O + S	O + S
<i>a</i> (Å)	3.05(2)	3.06(1)	3.06(1)	3.07(1)	3.08(1)	4.202(5)	4.201(2)	4.215(2)	4.220(4)	4.230(5)	4.256(2) 8.145(3)	4.267(2) 8.148(3)
<i>c</i> (Å)	23.2(1)	23.2(1)	22.96(1)	19.98(3)	19.91(3)							
<i>V</i> (Å ³)	187(2)	188(1)	186.4(2)	163.7(5)	163.1(4)	74.2(2)	74.1(1)	74.9(1)	75.2(2)	75.7(2)	77.1(1) 540.3(6)	77.7(1) 540.9(6)

^a HT = hydrotalcite like phase. O = mixed oxide phase. S = spinel type phase. The '*a*' lattice parameter of the mixed oxide phase is calculated on the basis of the MgO rock-salt structure.²⁹

TABLE 2: Chemical Composition, Refined Structural Parameters, and Agreement Indexes for the Ni/Mg/Al Mixed Oxides (esd in parentheses)

sample, Ni:Mg:Al ^a															
	1, 0:71:29			2, 10:61:29			3, 34:37:29			4, 61:10:29			5, 71:0:29		
	Cell Parameters ^b														
<i>a</i> (Å)	8.3761(6)			8.3622(6)			8.3193(4)			8.3114(4)			8.3084(4)		
<i>V</i> (Å ³)	587.6(2)			584.7(2)			575.7(2)			574.1(2)			573.5(1)		
	Oxygen Position ^c														
<i>x</i>	0.2501(6)			0.2479(7)			0.2476(8)			0.2514(5)			0.2504(5)		
	Agreement Indexes														
<i>R</i> _p	1.70			2.31			2.18			2.67			3.01		
<i>R</i> _{wp}	2.17			3.03			2.71			3.44			3.80		
	Occupation Factors ^d														
	sample 1			sample 2			sample 3			sample 4			sample 5		
site	16c	16d	8a	16c	16d	8a	16c	16d	8a	16c	16d	8a	16c	16d	8a
Ni							0.48(7)	0.78(4)		0.86(8)	0.66(6)		1.0(2)	0.66(6)	
Mg	0.42(5)	0.65(4)	0.24(3)	0.56(4)	0.70(3)	0.23(3)	0.52(7)		0.29(3)	0.14(8)					
Al	0.58(5)			0.44(4)								0.29(3)	0.0(2)		0.28(4)

^a Atomic ratio % of the HT precursor as evidenced from chemical analysis. ^b Refined value of the mixed oxide supercell (spinel type cell); see text for the details. ^c Oxygen fractional coordinate. ^d For each sample the three columns report, respectively, the OF, normalized to unity, of the 16c, 16d, and 8a crystallographic site of space group *Fd3m*. The presence of cation in the crystallographic site 8b was tested, but the OF were close to zero. For this reason the OF of the site 8b has been fixed equal to zero and it is not reported in the table.

23.9° decrease progressively below 500 K and then dramatically between 500 and 550 K. These changes correspond to a decrease in the interplanar distances. The (1 1 0) and (1 1 3) reflections (located at a 2θ of about 64°) on the other hand show a slight shift toward longer distances between RT and 600 K. These observations are consistent with the expulsion of the water present between the Mg/Al hydroxide layers of the HT structure at 500 K^{5,10,12} together with the thermal expansion of the unit cell. The loss of water above 500 K leads to a contraction of the *c*-axis without the disruption of the layered HT structure, but above 600 K the latter disintegrates and carbon dioxide and water are evolved.^{10,12,13} Novel modifications to the intensities of the reflections that accompany these changes are reported.

The intensity of the (0 0 6) reflection decreases progressively by up to 50% between RT and 500 K. Contrary to observations made using X-ray diffraction and other methods,^{10,12} the reflection does not disappear at 500 K, but instead, its intensity drops sharply. This is accompanied by a broadening of the total intensity of a group of peaks at *ca.* $2\theta = 47.7^\circ$ because of the superimposition of some reflections that shift independently of one another with temperature. The intensity of the reflection at $2\theta = 68^\circ$ (corresponding to the (1 1 6) plane) decreases, ending ultimately with the disappearance of the peak at 550 K.

The unit cell data of the various phases at the different temperatures reported in Table 1 were obtained from the position of several reflections. The lattice parameter of the mixed oxide phases is calculated on the basis of the MgO rock-salt structure.²⁹

The data demonstrate the global effect of the expulsion of carbon dioxide and water from the HT structure on the lattice parameters. A small expansion of the *a*-axis and a contraction

of the *c*-axis are clearly discernible. The mixed oxides obtained from HT and the spinel to which it partially converts are poorly crystalline but this is reversed at higher temperatures. In addition, the data reveal the rate of thermal expansion for the various phases.

(b) Full Pattern Profile Refinements. Since the systems discussed in this paper have nonstoichiometric phases where the amorphous component is more often than not present in a relatively large amount, the diffraction patterns are not the most suitable to be investigated using conventional diffraction methods. Our approach, therefore, may represent an extreme application of the Rietveld method for interpreting the diffraction patterns.

Five Ni/Mg/Al HT samples with a molar ratio M(II)/M(III) of 2.5 and differing in chemical composition (see Table 2) were subjected to calcination at 923 K overnight and then cooled to room temperature before analysis. This temperature was chosen, since it could offer good quality data and at the same time facilitate an unambiguous interpretation of the diffraction pattern because of the absence of contamination from segregation of the spinel phase.^{10,15,17}

The full pattern refinements were carried out as discussed in section III above and based on the *Fm3m* (*n*.225) space group in which both MgO and NiO crystallize. The agreement indexes of the refinements were good, but the poor fitting to the reflection at $2\theta = 37.2^\circ$ ($d = 2.50$ Å) and the presence of a new reflection at $2\theta = 18.8^\circ$ ($d = 4.88$ Å) for the nickel-richest samples (samples 4 and 5) led us to propose the coexistence of a small amount of spinel with the oxide phase. The refinements carried out on the basis of a two-phase system (i.e., oxide and

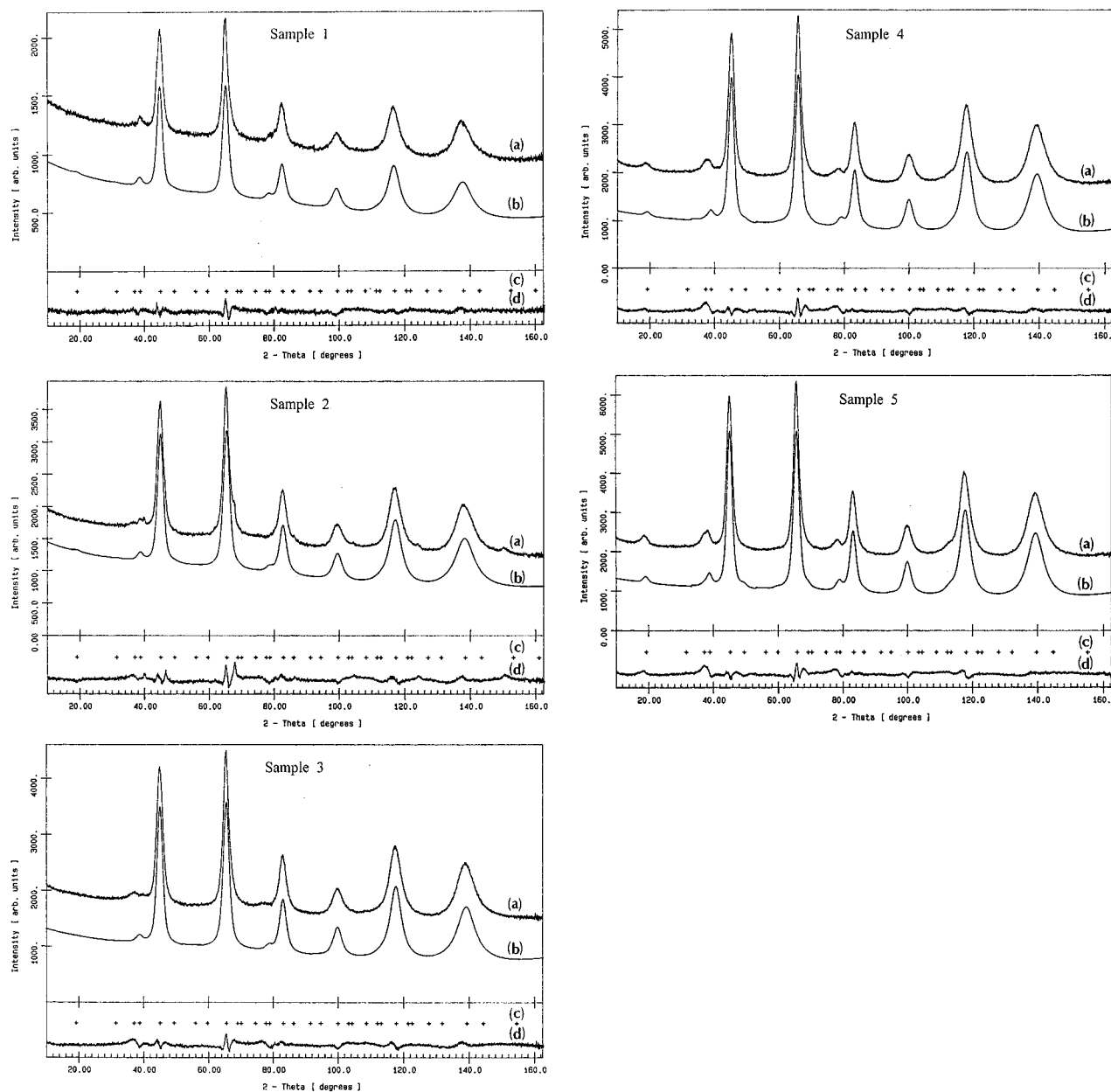


Figure 3. Comparison between the observed (a) and calculated (b) neutron powder patterns of the different samples obtained by calcination of HT at 923 K. The crosses (c) are the reflection position markers, and the bottom curve (d) is the difference profile.

spinel) gave very poor results, since the introduction of a second phase resulted in an improvement of the fitting of the reflections at $2\theta = 18.8^\circ$ and $2\theta = 37.2^\circ$ but invariably generated peaks at larger 2θ angles that had not been observed experimentally. The hexagonal distorted model for the NiO structure^{30,31} was also tested without success.

Because of the possible intimate coexistence of the MgO and the spinel phases, due to the close relationship between their structures, the refinements were then performed using a more flexible model that allowed the use of parameters based on a spinel phase. MgO and spinel have the same framework of oxygen atoms that essentially differ in (i) the "a" unit cell parameter—the spinel cell axis is almost twice the oxide one (e.g., 8.083 Å in MgAl_2O_4 compared to 4.213 Å in MgO)^{29,32}—and (ii) the location of the cations and the degree of filling of the cavities associated with the oxygen atoms by the former. The spinel unit cell contains 32O^{2-} ions in cubic close packing defining 32 octahedral and 64 tetrahedral interstices. Of these, only an eighth of the tetrahedral (crystallographic site 8a^{33,34}) and a half of the octahedral (site 16c^{33,34})

are occupied in a stoichiometric MgAl_2O_4 spinel. Therefore, the spinel structure has a lot of empty sites in which many ions can be accommodated.

On the other hand, the Mg/Ni/O phase unit cell contains four oxygen atoms and four crystallographically equivalent metal atoms octahedrally coordinated giving rise to the so-called rock-salt type structure. Nonstoichiometric spinels show structures that are between the spinel and rock-salt types. The rock-salt oxide lattice can be described using a supercell with a lattice parameter twice that of the oxide and the scaled down coordinates reported for the stoichiometric spinel space group $Fd3m$ (n.227).³⁴ The unit cell volume increases 8-fold compared with that of the original cell. The oxide supercell contains 32 oxygen atoms and 32 cations that fill all the octahedrally coordinated positions. Owing to the $Fd3m$ space group symmetry rules,³⁵ the octahedral sites are nonequivalent and are identified as 16c and 16d. In stoichiometric MgAl_2O_4 , Al atoms occupy the 16c site, the 16d site is empty, while the Mg atoms occupy the tetrahedrally coordinated positions (site 8a). The last of these sites is empty in rock-salt structure like MgO. In

other spinels the distribution of the cations in the interstices may be different (e.g., sites 16c empty and 16d filled like in a crystalline form of Co_3O_4 ³⁶).

The flexible structural model used by us is a spinel (cell parameter twice relative to the rock-salt oxide) in the space group $Fd3m$ and the possibility of having cations in the octahedral 16c, 16d, and tetrahedral 8a, 8b is verified.

The results of the refinements are shown in Table 2 and the comparisons between the observed and calculated neutron diffraction patterns are reported in Figure 3.

At first, let us consider the results of the simplest samples (1 and 5) in which only two cations are present. The data in Table 2 reveal that in the case of sample 5 (based on Ni/Al), the 16c sites are filled completely with Ni atoms and that there is no replacement with aluminium as is the case in previous refinements based on a simplified model.¹⁵ On the other hand the Mg/Al sample 1 shows a high degree ($58 \pm 5\%$) of aluminium substitution for Mg atoms at site 16c relatively to the MgO structure. The OF of site 16d were calculated without the imposition of any constraint, and both samples 1 and 5 showed a considerable degree ($35 \pm 2\%$) of vacancy in this position. Finally, Mg and Al atoms were used to test the presence of metals in site 8a in samples 1 and 5, respectively. There were no constraints imposed with the result that about a quarter were filled by cations in both the samples.

It must be pointed out that when there is a considerable amount of vacancy together with the possibility of a certain degree of atom substitution in a crystal site, the refinement cannot give real information on the chemical species involved. The aluminium was used for the Ni-richest sample (sample 5) in view of the high degree of inversion observed for the nickel aluminate.³⁷ For the Mg-richest sample (sample 1), the magnesium was used because the magnesium spinel is normal. Some runs were carried out using Al for sample 1 and Ni for sample 5 with the conclusion that, although the numerical result depends on the atom used, only a fraction of the 8a sites is filled in both binary samples 1 and 5. Indeed,²⁷ Al NMR studies suggest that tetrahedrally coordinated aluminium atoms are present in Mg/Al systems.^{10,13,14} The presence of cation atoms in a tetrahedral site of Mg/Al mixed oxides agrees with the model hypothesized by Rebour *et al.*^{10,14} who, because of the limitations inherent in X-ray diffraction, could not make use of the Rietveld method.

Refinements of the data for the samples with intermediate composition (samples 2–4) proceeded with increasing complexity (because of multiple substitutions) *via* the approach employed for samples 1 and 5. In order to reduce the number of variables, the Mg/Ni ratio of each sample (Table 2) was used to normalize corresponding chemical compositions, and because site 16c is completely filled with rock-salt and spinel structures, a complete filling of the site was assumed. Only at the end of the refining procedure was the relative amount of the divalent cations allowed to vary in order to test the validity of the above assumption. For samples 3 and 4 the Mg/Ni ratio oscillated around the imposed values without any significant effect on other variables, but in the case of sample 2, the OF of Ni atoms were reduced to zero. The refinement of sample 2 data was therefore performed with the possibility of aluminium substitution for magnesium in site 16c. The $44 \pm 4\%$ of magnesium positions were occupied by Al atoms. That indicates that Ni atoms are possibly allocated in the 16d site.

The OF of the 16d site for samples 2–4 were refined without constraints using only one atomic species as a probe. Rietveld refinements reveal that for all samples there exists a neutron density deficiency ascribable to either cation vacancy or

substitution of magnesium or nickel with cations with lower scattering power (aluminium or magnesium or both). The presence of a number of vacancies at this site is expected, since the structure tends toward a spinel phase in which there are no atoms in the site 16d. The phenomenon can be attributed to the onset of ion migration toward other positions. Although the value reported in Table 2 for site 16d is strictly dependent on the probe atom, it should be noted that the results obtained from refinements show that the oxides under investigation contain a fraction of empty octahedral sites.

The factors associated with the vacancies are also applicable to the 8a site. Assuming the presence of Mg atoms in site 8a for samples 2 and 3 or Al atoms for sample 4 during the test for the presence of residual neutron density, a small fraction of cations were generated in the tetrahedral position (Table 2). Owing to the high degree of vacancies, it is not possible to comment on the true chemical species involved.

The refined supercell *a*-axes are reported in Table 2. For sample 1, $a = 8.3761 \pm 0.0006 \text{ \AA}$ can be compared to twice the one of MgO ($a = 4.213 \text{ \AA}$)²⁹ and the one for sample 5 ($a = 8.3084 \pm 0.0004 \text{ \AA}$) to twice that of NiO ($a = 4.177 \text{ \AA}$).³⁸ Although the differences are very slight, the trend toward a contraction of the supercell can be invoked as further evidence of the partial evolution of the system toward a spinel-like structure.

V. Conclusions

The *in situ* temperature neutron diffraction analysis performed on the HT sample $[\text{Mg}_{0.71}\text{Al}_{0.29}(\text{OH})_2(\text{CO}_3)_{0.145} \cdot m\text{H}_2\text{O}]$ has provided considerable insight into the structural changes that take place between RT and 1250 K. The evolution from a HT phase to a mixed oxide one leading to the partial segregation to a spinel phase is clearly evident. The structural modifications that occur around 500 K are associated with the interlayer water loss and are related not only to the contraction of the *c*-axis parameter but also to other numerous changes embodied in the various peaks in the neutron diffraction patterns.

The Rietveld refinements carried out on the data from the five Ni/Mg/Al mixed oxides that had been obtained by calcination of HT at 923 K indicate that a structural model that takes into account the presence of cations in the tetrahedral position can be invoked in all cases. On the basis of the results, one concludes that although the oxide phases show diffraction patterns similar to those of a mixed rock-salt phase, the lattice is far from ideal.

The main deviations from the idealized rock-salt stoichiometric phase are the presence of (i) a supercell with the *a*-axis twice that of the stoichiometric oxide (a spinel type cell), (ii) a certain degree of cation vacancies in the octahedral 16d site, (iii) partial filling of the tetrahedral site 8a, and (iv) partial substitution of aluminium for magnesium in magnesium-rich samples. It must be pointed out that these results can be attributed to a defective spinel-like structure proposed previously for Ni/Al and Ni/Mg/Al mixed oxide systems obtained from hydrotalcite decomposition, based on selective leaching experiments using concentrated NaOH.^{39–42}

Acknowledgment. The authors thank Dr. Paolo Radaelli and Mr. Peter Cross (ILL, Grenoble) for scientific and technical support during the experiments and ILL for beam-time allocation. The financial support from Ministero per l'Università e la Ricerca Scientifica e Tecnologica (Italy) is gratefully acknowledged.

Supporting Information Available: One table listing chemical composition and nonstructural parameters (1 page). Ordering information is given on any current masthead page.

References and Notes

- (1) Dadyburiar, D. D.; Jewur, S. S.; Ruckenstein, E. *Catal. Rev. Sci. Eng.* **1979**, *19*, 293.
- (2) Lew, S.; Jothimurugesan, K.; Flytzani-Stephanopoulos, M. *Ind. Eng. Chem. Res.* **1989**, *28*, 535.
- (3) Suresh, K.; Kumar, N. R. S.; Patil, K. C. *Adv. Mater.* **1991**, *3*, 148.
- (4) Trifirò, F.; Vaccari, A.; Clause, O.; Gazzano, M. In *Euromat 91. Advanced Devices and Techniques*; Clyne, T. W., Withers, P. J., Eds.; The Institute of Materials: London, 1992; Vol. 3, p 304.
- (5) Cavani F.; Trifirò, F.; Vaccari A. *Catal. Today* **1991**, *11*, 173, and references therein.
- (6) Reichle, W. T. *CHEMTECH* **1986**, *16*, 58.
- (7) Trifirò, F.; Vaccari, A. In *Comprehensive Supramolecular Chemistry*; Atwood, J. L., et al., Eds.; Pergamon: Oxford, 1996; Vol. 7, p 251.
- (8) Kagunya, W. W. *J. Phys. Chem.* **1996**, *100*, 327.
- (9) Bellotto, M.; Rebours, B.; Clause, O.; Lynch, J.; Bazin, D.; Elkaïm, E. *J. Phys. Chem.* **1996**, *100*, 8527.
- (10) Bellotto, M.; Rebours, B.; Clause, O.; Lynch, J.; Bazin, D.; Elkaïm, E. *J. Phys. Chem.* **1996**, *100*, 8535.
- (11) Kagunya, W.; Hassan, Z.; Jones, W. *Inorg. Chem.* **1996**, *35*, 5970.
- (12) Pestic, L.; Salipurovic, S.; Markovic, V.; Vucelic, D.; Kagunya, W.; Jones, W. *J. Mater. Chem.* **1992**, *2*, 1992.
- (13) Rey, F.; Fornes V.; Rojo, J. M. *J. Chem. Soc., Faraday Trans. 1* **1992**, *88*, 2233.
- (14) Rebours, B.; D'Espinose de la Caillerie, J. B.; Clause, O. *J. Am. Chem. Soc.* **1994**, *116*, 1707.
- (15) Vaccari, A.; Gazzano, M. In *Preparation of Catalysts VI*; Poncelet, G., et al., Eds.; Elsevier: Amsterdam, 1995; p 893.
- (16) Shen, J.; Kobe, J. M.; Chen, Y.; Dumesic, J. A. *Langmuir* **1994**, *10*, 3902.
- (17) Clause, O.; Gazzano, M.; Trifirò, F.; Vaccari, A.; Zatorski, L. *Appl. Catal.* **1991**, *73*, 217.
- (18) Derouane, E. G.; Davis, R. G.; Blom, N. J. Eur. Pat. Appl. EP 476489, 1992.
- (19) Derouane, E. G.; Jullien-Lardot, V.; Davis, R. J.; Blom, N.; Hojlund-Nielsen, P. E. *New Frontiers in Catalysis*; Gucci, L., et al., Eds.; Academia Kiado: Budapest, 1993; Vol. B, p 1031.
- (20) Rostrup-Nielsen, J. R. *J. Catal.* **1974**, *33*, 184.
- (21) Gadalla, A. M.; Sommer, M. E. *J. Am. Ceram. Soc.* **1979**, *72*, 683.
- (22) Basile, F.; Basini, L.; Fornasari, F.; Matteuzzi, D.; Trifirò, F.; Vaccari, A. In *Actas XV Simp. Iberoamericano de Catalysis*; Herrero, E., et al., Eds.; Universidad Nacional de Córdoba: Córdoba, Argentina, 1996; Vol. 3, p 1843.
- (23) Hewat, A. W. In *High Resolution Powder Diffraction, Materials Research Forum*; Catlow, C. R. A., Ed.; Trans Tech Publications: Zürich, 1986; p 69.
- (24) Rietveld, H. M. *Acta Crystallogr.* **1967**, *22*, 151.
- (25) Rietveld, H. M. *J. Appl. Crystallogr.* **1969**, *2*, 65.
- (26) Wiles, D. B.; Young, R. A. *J. Appl. Crystallogr.* **1981**, *14*, 149.
- (27) *International Tables for X-ray Crystallography*; Kynoch Press: Birmingham, U.K., 1974; Vol. IV.
- (28) Sasaki, S.; Fujino, K.; Takeuchi, Y. *Proc. Jpn. Acad.* **1979**, *55*, 43.
- (29) International Center for Diffraction Data, File No. 4-829, Newton Square, PA.
- (30) Rooksby, H. P. *Acta Crystallogr.* **1948**, *1*, 226.
- (31) Massarotti, V.; Capsoni, D.; Berbenni, V.; Riccardi, R.; Marini, A.; Antolini, E. *Z. Naturforsch.* **1991**, *46A* 503.
- (32) International Center for Diffraction Data, File No. 21-1152, Newton Square, PA.
- (33) Wells A. F. In *Structural Inorganic Chemistry*; Oxford University Press: Oxford, 1984; p 592.
- (34) Wyckoff, R. W. G. In *Crystal Structures*; Interscience Publishers: New York, 1968; Vol. 4, p 76.
- (35) *International Tables for X-ray Crystallography*; Kynoch Press: Birmingham, U.K., 1974; Vol. I.
- (36) Smith, W. L.; Hobson, A. D. *Acta Crystallogr.* **1973**, *B29*, 362.
- (37) Roelofsen, J. N.; Peterson, R. C.; Raudsepp, M. *Am. Mineral.* **1992**, *77*, 522.
- (38) International Center for Diffraction Data, File No. 4-835, Newton Square, PA.
- (39) Sinha, K. P.; Sinha, P. B. *J. Phys. Chem.* **1957**, *61*, 758.
- (40) Clause, O.; Rebours, B.; Merlin, E.; Trifirò, F.; Vaccari, A. *J. Catal.* **1992**, *133*, 231.
- (41) Beccat, F.; Roussel, J. C.; Clause, O.; Vaccari, A.; Trifirò, F. In *Catalysis and Surface Characterization*; Dines, T. J., et al., Eds.; Royal Society of Chemistry: London, 1992; p 32.
- (42) Fornasari, G.; Gazzano, M.; Matteuzzi, D.; Trifirò, F.; Vaccari, A. *Appl. Clay Sci.* **1995**, *10*, 69.